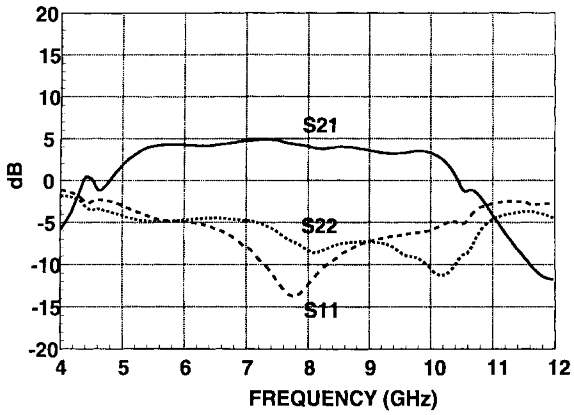

Fig. 5. Measured gain and return losses of the 5.4–10-GHz amplifier.

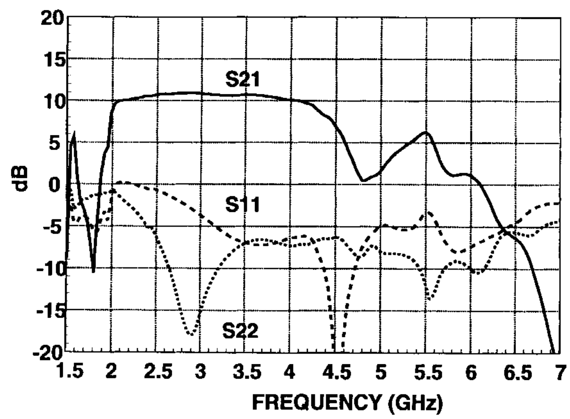

Fig. 6. Measured gain and return losses of the 2–4-GHz amplifier.

IV. Amplifier Performance

The new uniplanar push–pull amplifiers were fabricated on 1.27-mm RT/Duroid 6006, having a relative dielectric constant of 6.15. Figs. 4 and 5 show the calculated and measured gains (S_{21}) and input (S_{11}) and output (S_{22}) return losses of the first amplifier, respectively, designed using NE76184AS. The calculated magnitude of S_{11} is greater than 0 dB below 5 GHz, indicating a potential instability problem in the amplifier. This was expected as this transistor is only unconditionally stable from 6 to 11 GHz. The measured gain is between 3.5–5 dB from 5.4 to 10 GHz. Fig. 6 shows the measured gain and input and output return losses of the other amplifier using NE76084AS. The gain is between 10 and 11 dB from 2 to 4 GHz. As seen in Figs. 4 and 5, the measured and computed results for the 5.4–10 GHz amplifier are not in a good agreement. A similar discrepancy was seen for the 2–4-GHz amplifier. These discrepancies were expected because many approximations were involved in the design process; for example, the effects of the discontinuities in the uniplanar circuits and the transitions used in the baluns were not taken into account in the circuit simulations. In addition, we used the S-parameters of the FET's from the data manual which do not represent accurately the S-parameters of the actual devices used. It should be noted here that the discontinuities and transitions can be accurately modeled using full-wave methods, and the FET's used can also be accurately represented by measuring their S-parameters. These accurate models can then be used to achieve a much better agreement between the amplifiers' experimental and simulated results. However, these are beyond the scope of this paper, as our purpose is to demonstrate the feasibility of the proposed amplifier configuration. The measured output 1-dB compression points of the 2–4 GHz and 5.4–10-GHz amplifiers are 17 dBm at 4 GHz and 19 dBm at 10 GHz, respectively.

V. Conclusions

New broad-band push–pull FET amplifiers have been developed. These amplifiers employ CPW and slot line and are completely uniplanar. One amplifier exhibits a gain of 3.5–5 dB over 5.4–10 GHz and an output 1-dB compression point of 19 dBm at 10 GHz. The other amplifier has a measured gain from 10 to 11 dB over 2–4 GHz and an output 1-dB compression point of 17 dBm at 4 GHz. These amplifiers demonstrate a successful implementation of the push–pull amplifier configuration using uniplanar technology for MIC's and MMIC's.

Acknowledgment

The authors wish to thank L. Fan and M. Li for their technical support. They also are grateful to the anonymous reviewers for their valuable comments and suggestions.

References

[1] C. H. Ho, L. Fan, and K. Chang, "New uniplanar coplanar waveguide hybrid-ring couplers and magic-T's," *IEEE Trans. Microwave Theory Tech.*, vol. 42, pp. 2440–2448, Dec. 1994.

[2] S. A. Maas, *Nonlinear Microwave Circuits.* Norwood, MA: Artech House, 1988.

The Method of Lines for the Hybrid Analysis of Multilayered Cylindrical Resonator Structures

Dennis Kremer and Reinhold Pregla

***Abstract*—A very powerful numerical model based on the method of lines (MoL) is developed for the hybrid analysis of composite multilayered cylindrical dielectric resonator structures. These structures are composed of a number of coaxial rings which are arbitrarily layered in the axial direction. The resonant frequencies, as well as quality factors caused by radiation or dielectric loss and the corresponding field distributions of all resonant modes can be determined with the described algorithm. The theory is verified in case of the conical dielectric resonator and a comparison of our numerical results with those of other authors shows excellent consistency.**

***Index Terms*—Conical resonator, MoL, multilayered cylindrical dielectric resonators.**

Manuscript received June 27, 1996; revised December 1, 1996.

D. Kremer was with Allgemeine/Theoretische Elektrotechnik, Fern Universitaet, D-58084 Hagen, Germany. He is now with E-Plus Mobilfunk GmbH, D-40468 Düsseldorf, Germany.

R. Pregla is with Allgemeine/Theoretische Elektrotechnik, FernUniversität, D-58084 Hagen, Germany.

Publisher Item Identifier S 0018-9480(97)08238-0.

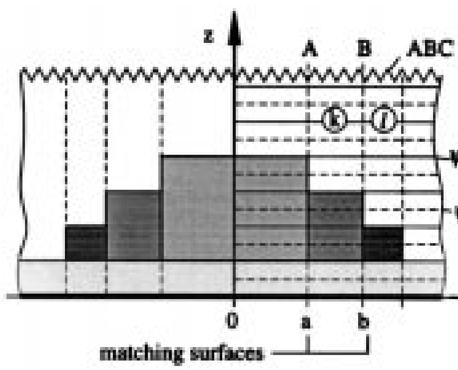

Fig. 1. Discretization of a composite multilayered resonator structure.

I. INTRODUCTION

In integrated microwave engineering, resonators are utilized in a variety of applications, including filter elements, the stabilization of oscillators, frequency meters, and tuned amplifiers. The necessity of reducing the cost of microwave circuits makes the reduction of their size essential. In this respect, the low-cost dielectric resonators became more and more important in telecommunication and satellite communication. The increasing importance of mobile telecommunication systems and the shift from vehicle-mounted mobile-phone systems to portable units has especially increased the demand for dielectric resonators which are compact, reasonably priced, and have good temperature stability. Due to the proximity of the resonant frequencies of the various hybrid modes to one another, it is very important to know all the exact resonant frequencies and the corresponding field distributions in the frequency range of interest. Currently, there are several approaches available for the rigorous analysis of cylindrical dielectric resonators [1]. Most of them are only useful for the determination of resonator modes without azimuthal variations or are restricted to particular geometries. The method of moments based on the surface integral equation [2], [3], the null-field method [4], and a combination of the finite-difference time-domain and Prony's method [5] have been further developed to enable the hybrid analysis of isolated dielectric resonators. It has been shown in a number of papers that the method of lines (MoL) [6] is highly suitable for the analysis of electromagnetic field problems. The MoL is a semianalytical method in which the relevant wave equations are discretized only in one or two directions and solved analytically in the remaining directions. The MoL behaves stationary and, therefore, the convergence curves are monotonic [7] making an extrapolation to the accurate result possible. This leads to results with a high degree of accuracy with less computational effort. The introduction of absorbing boundary conditions in the MoL has made it possible to simulate radiating structures such as microstrip patch antennas [8] and cylindrical antennas [9].

The purpose of this paper is to show that the MoL can be applied very efficiently to the analysis of resonator structures in the cylindrical coordinate system. Our model enables us to investigate resonator structures with different shapes, e.g., rotationally symmetric, cylindrical, or conical forms placed on a substrate. In [10], an isolated dielectric resonator with a cylindrical form was analyzed and it could be demonstrated that our model is very accurate. This model can be modified very easily making the analysis of structures possible which include metal layers like microstrip ring resonators with the same algorithm. As a surrounding boundary of the structure, we can use either absorbing boundary conditions, metallic, or magnetic walls. The resonator structure is modeled by a set of single coaxial rings in the radial direction. These rings show permittivities that depend on the z-direction. Lossy materials can be considered using complex permittivities. Such multilayered dielectric resonators surrounded by metallic walls were first investigated by [11] using an algorithm based on the mode-matching technique and [12] with a differential method.

II. THEORY

In cylindrical coordinates, the electromagnetic field for an inhomogeneous dielectric medium can be determined by two vector potentials Π_e and Π_h, each one having only one component ψ_e and ψ_h in the z-direction, respectively. If we assume a harmonic time-dependence in accordance with $e^{j\omega t}$ and a space dependence of the permittivity according to $\varepsilon_r(z)$, the scalar potentials ψ_e and ψ_h must fulfill the Sturm–Liouville differential equation and the Helmholtz equation in cylindrical coordinates, respectively,

$$\frac{1}{\overline{r}}\frac{\partial}{\partial\overline{r}}\left(\overline{r}\,\frac{\partial\psi_e}{\partial\overline{r}}\right)+\frac{1}{\overline{r}^2}\,\frac{\partial^2\psi_e}{\partial\varphi^2}+\varepsilon_r\,\frac{\partial}{\partial\overline{z}}\left(\varepsilon_r^{-1}\,\frac{\partial\psi_e}{\partial\overline{z}}\right)+\varepsilon_r\psi_e=0 \quad (1)$$

$$\frac{1}{\overline{r}}\frac{\partial}{\partial\overline{r}}\left(\overline{r}\,\frac{\partial\psi_h}{\partial\overline{r}}\right)+\frac{1}{\overline{r}^2}\,\frac{\partial^2\psi_h}{\partial\varphi^2}+\frac{\partial^2\psi_h}{\partial\overline{z}^2}+\varepsilon_r\psi_h=0 \quad (2)$$

$\overline{r}=k_o r$ and $\overline{z}=k_o z$ are the normalized coordinates and k_o is the free-space wavenumber. For resonator structures, which are rotationally symmetric, we get the relation

$$\frac{\partial^2\psi_{e,h}}{\partial\varphi^2}=-m^2\psi_{e,h} \quad (3)$$

with the mode order m in azimuthal direction. To solve the two differential equations in (1) and (2) the potentials and the permittivities ε are partly discretized perpendicular to the axis of rotation. Fig. 1 shows the longitudinal section of the discretized computational window. As the discretization is only enforced in the z-direction, the potentials and fields are analytically calculated on lines in the radial direction. We use two different line systems for the potentials ψ_e and ψ_h, which are shifted toward each other to satisfy the interface conditions in the discretization direction. According to the explanations in [6] concerning the derivations on the two line systems we obtain the following formulas:

$$\begin{aligned}\overline{h}\,\frac{\partial\psi_h}{\partial\overline{z}}&\rightarrow\boldsymbol{D}_a\boldsymbol{\psi}_h\\ \overline{h}\,\frac{\partial\psi_e}{\partial\overline{z}}&\rightarrow-\boldsymbol{D}^t\boldsymbol{\psi}_e\\ \overline{h}^2\,\frac{\partial^2\psi_h}{\partial\overline{z}^2}&\rightarrow-\boldsymbol{D}^t\boldsymbol{D}_a\boldsymbol{\psi}_h=-\boldsymbol{P}_h\boldsymbol{\psi}_h\\ \overline{h}^2\varepsilon_r(z)\,\frac{\partial}{\partial\overline{z}}\left(\varepsilon_r^{-1}(z)\,\frac{\partial\psi_e}{\partial\overline{z}}\right)&\rightarrow-\boldsymbol{\epsilon}_e\boldsymbol{D}_a\boldsymbol{\epsilon}_h^{-1}\boldsymbol{D}^t\boldsymbol{\psi}_e=-\boldsymbol{P}_e\boldsymbol{\psi}_e\end{aligned} \quad (4)$$

ψ_e and ψ_h are column vectors composed of the discretized potentials; $\boldsymbol{\epsilon}_e$ and $\boldsymbol{\epsilon}_h$ denote diagonal matrices containing the values of the permittivity on the distinct line system. Substituting the corresponding difference operators in place of the differential operators in (1) and (2) results in two sets of coupled differential equations. After decoupling these equations by transforming them to the main axis, we obtain a system of uncoupled differential equations for the transformed potentials $\tilde{\boldsymbol{\psi}}_{e,h}$:

$$\overline{r}\,\frac{\partial}{\partial\overline{r}}\left(\overline{r}\,\frac{\partial\tilde{\boldsymbol{\psi}}_{e,h}}{\partial\overline{r}}\right)+[(\boldsymbol{k}_{re,h}\overline{r})^2-m^2\boldsymbol{I}_{e,h}]\tilde{\boldsymbol{\psi}}_{e,h}=\boldsymbol{0} \quad (5)$$

with

$$\boldsymbol{T}_{e,h}^{-1}\underbrace{(\boldsymbol{\epsilon}_{e,h}-\boldsymbol{P}_{e,h})}_{\boldsymbol{Q}_{e,h}}\boldsymbol{T}_{e,h}=\boldsymbol{k}_{r_{e,h}}^2$$

and

$$\boldsymbol{\psi}_{e,h}=\boldsymbol{T}_{e,h}\tilde{\boldsymbol{\psi}}_{e,h}.$$

The matrices $\boldsymbol{k}_{re}$ and $\boldsymbol{k}_{rh}$ contain the propagation constant in the radial direction on the main diagonal. $\boldsymbol{T}_e$ and $\boldsymbol{T}_h$ are the transformation matrices. $\boldsymbol{P}_e$ and $\boldsymbol{P}_h$ are the difference operators for the second derivatives according to (4). As a general solution of the uncoupled differential equations a linear combination of the Bessel function of the first and the second kind according to

$$\tilde{\boldsymbol{\psi}}_{e,h} = J_m(\boldsymbol{k}_{r_{e,h}}\overline{r})\boldsymbol{A}_{e,h} + Y_m(\boldsymbol{k}_{r_{e,h}}\overline{r})\boldsymbol{B}_{e,h} \tag{6}$$

can be used. This solution enables us to transfer the quantities readily from one side of a layer to the other. For the normalized radii $\overline{r} = \overline{a}$ and $\overline{r} = \overline{b}$ we can use the following matrix form:

$$\begin{bmatrix}\tilde{\boldsymbol{\psi}}_A \\ \tilde{\boldsymbol{\psi}}_B\end{bmatrix} = \begin{bmatrix}J_m(\boldsymbol{k}_{r_{e,h}}\overline{a}) & Y_m(\boldsymbol{k}_{r_{e,h}}\overline{a}) \\ J_m(\boldsymbol{k}_{r_{e,h}}\overline{b}) & Y_m(\boldsymbol{k}_{r_{e,h}}\overline{b})\end{bmatrix}\begin{bmatrix}\boldsymbol{A} \\ \boldsymbol{B}\end{bmatrix} \tag{7}$$

and the derivative to $\overline{r}$ can be expressed by

$$\overline{r}\,\frac{\partial}{\partial \overline{r}}\begin{bmatrix}\tilde{\boldsymbol{\psi}}_A \\ \tilde{\boldsymbol{\psi}}_B\end{bmatrix} = \hat{\boldsymbol{p}}_m^{-1}\begin{bmatrix}\overline{\boldsymbol{r}}_m & \frac{2}{\pi}\boldsymbol{I} \\ -\frac{2}{\pi}\boldsymbol{I} & \overline{\boldsymbol{q}}_m\end{bmatrix}\begin{bmatrix}\tilde{\boldsymbol{\psi}}_A \\ \tilde{\boldsymbol{\psi}}_B\end{bmatrix} \tag{8}$$

$\hat{\boldsymbol{p}}_m$ is a block diagonal matrix composed by the matrices $\boldsymbol{p}_m$. The detailed structure of the normalized cross-products used here can be found in Appendix A. After some algebraic manipulations, we obtain the following system of equations for the tangential-field components on the cylinder planes A and B:

$$\begin{bmatrix}\boldsymbol{H}_A \\ \boldsymbol{H}_B\end{bmatrix} = \begin{bmatrix}\boldsymbol{y}_{1A} & \boldsymbol{y}_2 \\ \boldsymbol{y}_2 & \boldsymbol{y}_{1B}\end{bmatrix}\begin{bmatrix}\boldsymbol{E}_A \\ -\boldsymbol{E}_B\end{bmatrix} \tag{9}$$

with the abbreviations

$$\boldsymbol{H}_{A,B} = j\eta_o\begin{bmatrix}\boldsymbol{H}_{zA,B} \\ \overline{r}_{A,B}\boldsymbol{H}_{\varphi A,B}\end{bmatrix} \quad \boldsymbol{E}_{A,B} = \begin{bmatrix}\overline{r}_{A,B}\boldsymbol{E}_{\varphi A,B} \\ \boldsymbol{E}_{zA,B}\end{bmatrix}. \tag{10}$$

The detailed compositions of the matrices $\boldsymbol{y}_{1A}$, $\boldsymbol{y}_{1B}$, and $\boldsymbol{y}_2$ are specified in Appendix B. Formally, (9) is equivalent with [6, eq. (138)]. The further analysis can be carried out as described in detail in [13]. Only the recurrence relations differ somewhat. For the transformation from the inner to the outer side we have to use

$$\boldsymbol{Y}_t^{(k)} = \boldsymbol{y}_2(\boldsymbol{y}_{1A} - \boldsymbol{Y}_t^{(k-1)})^{-1}\boldsymbol{y}_2 - \boldsymbol{y}_{1B} \tag{11}$$

and for the transformation from the outer to the inner side

$$\boldsymbol{Y}_t^{(l)} = \boldsymbol{y}_2(\boldsymbol{y}_{1B} - \boldsymbol{Y}_t^{(l-1)})^{-1}\boldsymbol{y}_2 - \boldsymbol{y}_{1A} \tag{12}$$

respectively. Matching the tangential field components at the interfaces of the cylindrical rings yields an indirect eigenvalue problem. This eigenvalue problem is similar to the one in [6], except that all matrices are now complex. This problem could be solved very efficiently by the MoL using the singular value decomposition (SVD) [14]. One advantage of the SVD is that we obtain a real function with complex frequencies as argument instead of a complex function with a complex argument. On the other hand, the field distribution in the matching plane is provided directly by one of the transformation matrices. For that very reason it is possible to decide what kind of mode was found.

III. Numerical Results

A conical dielectric resonator was analyzed with the algorithm demonstrated here, and the results were compared with those of [11]. In the radial direction, the shape of the cone was approximated by a set of single coaxial rings, which consist of inhomogeneous permittivities in z-direction. In Fig. 2, the resonant frequency of the TE_{011} mode is presented versus the height L. A comparison of our results with the numerical results in [11] shows that a very good consistency was achieved.

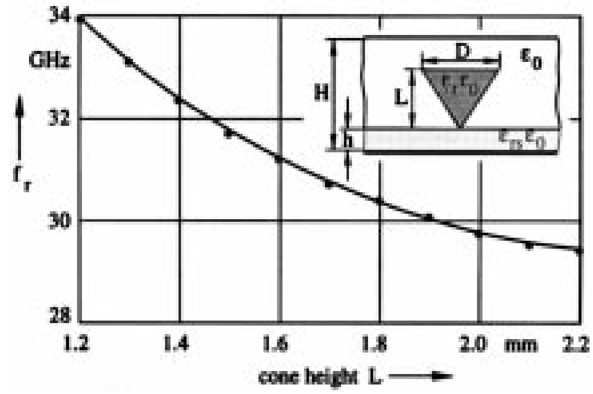

Fig. 2. Resonant frequency of the TE_{011} mode in a conical resonator with $D = 2.5$ mm, $H = 3.0$ mm, $h = 250\mu$m, $\epsilon_r = 29.57$, and $\epsilon_{rs} = 10$ versus cone height L (—theory [11], • MoL).

IV. Conclusion

A very powerful numerical model is developed for the hybrid analysis of dielectric resonator structures of complicated shape, such as the conical resonator. The computational model is based on the versatile MoL which has been proven to be very efficient for the analysis of a wide class of electromagnetic field problems. The algorithm developed makes the determination of resonant frequencies, quality factors, and field distributions for all resonant modes in a composite multilayered anisotropic dielectric resonator possible. Our numerical results have been compared with those of other authors and excellent agreement was achieved. As a consequence of the full vectorial analysis, the semianalytical, and the stationary character of the MoL our results were obtained with a high degree of accuracy and with less computational effort.

Appendix A

The normalized cross-products [15] used in (8) have the form

$$\begin{aligned}\boldsymbol{p}_m &= J_m(\boldsymbol{t}_A)Y_m(\boldsymbol{t}_B) - J_m(\boldsymbol{t}_B)Y_m(\boldsymbol{t}_A) \\ \overline{\boldsymbol{r}}_m &= \boldsymbol{t}_A[J_m'(\boldsymbol{t}_A)Y_m(\boldsymbol{t}_B) - Y_m'(\boldsymbol{t}_A)J_m(\boldsymbol{t}_B)] \\ \overline{\boldsymbol{q}}_m &= \boldsymbol{t}_B[J_m(\boldsymbol{t}_A)Y_m'(\boldsymbol{t}_B) - J_m'(\boldsymbol{t}_B)Y_m(\boldsymbol{t}_A)] \\ \overline{\boldsymbol{s}}_m &= \boldsymbol{t}_A\boldsymbol{t}_B[J_m'(\boldsymbol{t}_A)Y_m'(\boldsymbol{t}_B) - J_m'(\boldsymbol{t}_B)Y_m'(\boldsymbol{t}_A)]\end{aligned} \tag{13}$$

with $t_A = \boldsymbol{k}_r\overline{a}$ and $t_B = \boldsymbol{k}_r\overline{b}$.

Appendix B

For the sake of brevity, the following notations are used in (9):

$$\begin{aligned}\boldsymbol{y}_{1A} &= \begin{bmatrix}\boldsymbol{Q}_h\tilde{\boldsymbol{q}}_{mh} & \boldsymbol{Q}_h\tilde{\boldsymbol{q}}_{mh}\tilde{\boldsymbol{Q}}_e^{-1} \\ -\overline{\boldsymbol{D}}_a\tilde{\boldsymbol{q}}_{mh} & \gamma_{E1}\end{bmatrix} \\ \boldsymbol{y}_{1B} &= \begin{bmatrix}-\boldsymbol{Q}_h\tilde{\boldsymbol{r}}_{mh} & -\boldsymbol{Q}_h\tilde{\boldsymbol{r}}_{mh}\tilde{\boldsymbol{Q}}_e^{-1} \\ \overline{\boldsymbol{D}}_a\tilde{\boldsymbol{r}}_{mh} & -\gamma_{E2}\end{bmatrix} \\ \boldsymbol{y}_2 &= \begin{bmatrix}\boldsymbol{Q}_h\tilde{\boldsymbol{s}}_m^{-1} & \boldsymbol{Q}_h\tilde{\boldsymbol{s}}_m^{-1}\boldsymbol{Q}_e^{-1} \\ -\overline{\boldsymbol{D}}_a\tilde{\boldsymbol{s}}_m^{-1} & \boldsymbol{\alpha}_E\end{bmatrix}\end{aligned} \tag{14}$$

with

$$\begin{aligned}\tilde{\boldsymbol{Q}}_e^{-1} &= -\frac{m}{\overline{h}}\,\boldsymbol{\epsilon}_h^{-1}\boldsymbol{D}^t\boldsymbol{Q}_e^{-1}\boldsymbol{\epsilon}_e \\ \tilde{\boldsymbol{q}}_{mh} &= \boldsymbol{T}_h\boldsymbol{s}_{mh}^{-1}\overline{\boldsymbol{q}}_{mh}\boldsymbol{T}_h^{-1} \\ \tilde{\boldsymbol{s}}_m^{-1} &= \frac{2}{\pi}\,\boldsymbol{T}_h\boldsymbol{s}_{mh}^{-1}\boldsymbol{T}_h^{-1} \\ \tilde{\boldsymbol{r}}_{mh} &= \boldsymbol{T}_h\overline{\boldsymbol{r}}_{mh}\boldsymbol{T}_h^{-1} \\ \overline{\boldsymbol{D}}_a &= \frac{m}{\overline{h}}\,\boldsymbol{D}_a\end{aligned} \tag{15}$$

and

$$\begin{aligned} \boldsymbol{\gamma}_{E1} &= \boldsymbol{T}_e \boldsymbol{p}_{me}^{-1} \bar{\boldsymbol{r}}_{me} \boldsymbol{k}_{re}^{-2} \boldsymbol{T}_e^{-1} \boldsymbol{\epsilon}_e - \boldsymbol{Q}_h \tilde{\boldsymbol{q}}_{mh} \tilde{\boldsymbol{Q}}_e^{-1} \\ \boldsymbol{\alpha}_E &= -\frac{2}{\pi} \boldsymbol{T}_e \boldsymbol{p}_{me}^{-1} \boldsymbol{k}_{re}^{-2} \boldsymbol{T}_e^{-1} \boldsymbol{\epsilon}_e - \boldsymbol{Q}_h \tilde{\boldsymbol{s}}_m^{-1} \\ \boldsymbol{\gamma}_{E2} &= \boldsymbol{T}_e \boldsymbol{p}_{me}^{-1} \bar{\boldsymbol{q}}_{me} \boldsymbol{k}_{re}^{-2} \boldsymbol{T}_e^{-1} \boldsymbol{\epsilon}_e - \boldsymbol{T}_h \boldsymbol{k}_{r_h}^2 \boldsymbol{s}_{mh}^{-1} \bar{\boldsymbol{r}}_{mh} \boldsymbol{T}_e^{-1} \tilde{\boldsymbol{Q}}_e^{-1}. \end{aligned} \quad (16)$$

References

[1] D. Kajfez and P. Guillon, *Dielectric Resonators*. Norwood, MA: Artech House, 1986.

[2] D. Kajfez, A. W. Glisson, and J. James, "Computed modal field distributions for isolated dielectric resonators," *IEEE Trans. Microwave Theory Tech.*, vol. MTT-32, pp. 1609–1616, Dec. 1984.

[3] R. F. Harrington, *Field Computing by Moment Methods*. New York: Macmillian, 1968, ch. 3.

[4] W. Zheng, "Computation of complex resonance frequencies of isolated composite objects," *IEEE Trans. Microwave Theory Tech.*, vol. 37, pp. 953–961, June 1989.

[5] J. A. Pereda, L. A. Vielva, A. Vegas, and A. Prieto, "Computation of resonant frequencies and quality factors of open dielectric resonators by a combination of the finite-difference time-domain (FDTD) and Prony's methods," *IEEE Microwave Guided Wave Lett.*, vol. 2, pp. 431–433, Nov. 1992.

[6] R. Pregla and W. Pascher, "The method of lines," in *Numerical Techniques for Microwave and Millimeter Wave Passive Structures*, T. Itoh, Ed.. New York: Wiley, 1989, pp. 381–446.

[7] W. Hong and W.-X. Zhang, "On the equivalence between the method of lines and the variational method," *AEÜ*, vol. 45, pp. 198–201, 1991.

[8] A. Dreher and R. Pregla, "Full-wave analysis of radiating planar resonators with the method of lines," *IEEE Trans. Microwave Theory Tech.*, vol. 41, pp. 1363–1368, Aug. 1993.

[9] R. Pregla, "New approach for the analysis of cylindrical antennas by the method of lines," *Electron. Lett.*, vol. 30, no. 8, pp. 614–615, 1994.

[10] D. Kremer and R. Pregla, "The method of lines for the hybrid analysis of multilayered dielectric resonators," in *IEEE MTT-S Int. Symp. Dig.*, Orlando, FL, May 1995, pp. 491–494.

[11] W. K. Hui and I. Wolff, "A multicomposite, multilayered cylindrical dielectric resonator for application in MMIC's," in *IEEE MTT-S Int. Symp. Dig.*, Albuquerque, NM, May 1992, pp. 929–932.

[12] P. Vincent, "Computation of the resonant frequency of a dielectric resonator by a differential method," *Appl. Phys. A, Solids Surf.*, vol. 31, pp. 51–54, 1983.

[13] U. Rogge and R. Pregla, "Method of lines for the analysis of dielectric waveguides," *J. Lightwave Technol.*, vol. 11, pp. 2015–2020, Dec. 1993.

[14] D. Kremer, "Method of lines for the analysis of optical waveguide structures with complex refractive indices using a pole-free eigenvalue determination," *Electron. Lett.*, vol. 30, no. 13, pp. 1088–1089, June 1994.

[15] M. Abramowitz and I. A. Stegun, *Handbook of Mathematical Functions*. New York: Dover, 1965, ch. 9.

Nonradiating Sources in Time-Domain Transmission-Line Theory

Ari Sihvola, Gerhard Kristensson, and Ismo V. Lindell

***Abstract*—The concept of nonradiating (NR) sources is introduced to transmission lines in the time-domain analysis. A method is presented to construct localized voltage and current sources which do not produce any fields outside the source domain. These sources cannot, therefore, be detected by measurements made outside the source region. The importance of such sources for the uniqueness of the inverse-source problem is pointed out, and energy conditions for the uniqueness are discussed. The analysis can be advantageously used in the design and optimization of the electromagnetic compatibility (EMC) properties of transmission lines.**

***Index Terms*— Nonradiating sources, partial differential equations, transmission-line theory.**

I. Introduction

Direct problems in electromagnetics have unique solutions, which means that two different fields are necessarily generated by two different sources. However, the inverse problem is not unique without additional constraints. In other words, two different sources may radiate the same electromagnetic field outside the source region. One consequence of this nonuniqueness property of the inverse-source problem is that nonradiating (NR) sources exist. NR sources are such which do not generate any electric or magnetic fields outside their support.

The inverse-source problem in acoustics and electromagnetics has been studied by various authors [1], [3], [4], [7]. These papers treat currents and their radiation in free space from the NR point of view, and give conditions that the source distributions have to satisfy in order not to radiate electromagnetic energy. The construction of an NR-source distribution starts with choice of any function that vanishes outside a finite domain. Applying the wave operator to this function gives a certain source function. Because the resulting source function is a solution of the inhomogeneous-wave equation, it is an NR source because the field it corresponds to is zero outside the source domain.

One of the strong results of the NR-source studies is the following: a time-harmonic electric-current distribution $\mathbf{J}(\mathbf{r}, \omega)$ does not radiate electromagnetic fields outside its support if

$$\mathbf{k} \times \int \mathbf{J}(\mathbf{r}, \omega) e^{i\mathbf{k} \cdot \mathbf{r}} \, dV = 0 \quad (1)$$

for $\omega = c|\mathbf{k}|$. The integral behaves well because the integration domain is the support of the current distribution, which is a finite domain. In fact, (1) is a necessary and sufficient condition for a dynamic current to be NR. In other words, the NR condition is that certain components vanish of the transverse part of the spatial Fourier transform of the current density; namely those components for which $|\mathbf{k}| = \omega/c$, where $c = 1/\sqrt{\mu\epsilon}$ is the radiation velocity in the medium permeating the space [3]. To give one example of a single-frequency

Manuscript received October 17, 1996; revised August 22, 1997.

A. Sihvola is with the Department of Electromagnetic Theory, Lund Institute of Technology, S-221 00 Lund, Sweden, and the Helsinki University of Technology, Electromagnetics Laboratory, FIN-02015 HUT, Finland.

G. Kristensson is with the Department of Electromagnetic Theory, Lund Institute of Technology, S-221 00 Lund, Sweden.

I. V. Lindell is with the Helsinki University of Technology, Electromagnetics Laboratory, FIN-02015 HUT, Finland.

Publisher Item Identifier S 0018-9480(97)08249-5.